

- molecules were found and built into the structure. The ligand (29 atoms) was added in the final rounds of refinement with an occupancy of 0.50. The refinement (8.0 to 1.95 Å) rendered a final  $R_{\text{cryst}}$  for the model of 21.2% and a  $R_{\text{free}}$  of 26.1%. Root-mean-square deviations from ideal geometry for bond lengths were 0.008 Å, bond angles 1.6°, dihedral angles 25.7°, and improper angles 0.85°. All main-chain dihedral angles were in allowed regions of the Ramachandran plot, with 83% in the most favorable regions.
38. M. G. Ford *et al.*, *Science* **291**, 1051 (2001).
  39. P. C. Sternweis, A. V. Smrcka, *Trends Biochem. Sci.* **17**, 502 (1992).
  40. Constitutively active G-protein mutants. The following mutations ablate guanosine triphosphatase activity of the respective G proteins, resulting in constitutively active phenotypes:  $G_{\alpha_q}^*$ , Q209L;  $G_{\alpha_s}^*$ , Q227L;  $G_{\alpha_{11}}^*$ , Q209L;  $G_{\alpha_o}^*$ , Q205L.
  41. Tubby-G $\alpha$  coprecipitation assays. Recombinant GST-tubfl in the vector pEBG and untagged  $G_{\alpha_q}$  and  $G_{\alpha_o}$  in pCDNA3.1(-) were transiently overexpressed in 293T cells by calcium phosphate precipitation. Cells were harvested in PBS 36 hours after transfection and freeze-thawed once at room temperature. The pellets were resuspended in immunoprecipitation lysis buffer containing 20 mM Tris (pH 8.0), 1 M NaCl, 0.5% Nonidet P-40, 10% glycerol, 1 mM phenylmethylsulfonyl fluoride, 0.1  $\mu$ M aprotinin, 1  $\mu$ M leupeptin, and 1  $\mu$ l of pepstatin and incubated on ice for 30 min. After 30 strokes with a Dounce homogenizer, the cells were incubated for an additional 30 min, and then the lysate was cleared by centrifugation for 15 min at 16,000g at 4°C. A 20- $\mu$ l sample was removed for protein expression evaluation, and the remaining lysate was incubated on glutathione-Sepharose beads (Pharmacia 17-0756-01) for 2 hours at 4°C with gentle rotation. The complexes were washed four times with gentle vortexing in lysis buffer and resuspended in 2 $\times$  SDS-PAGE loading buffer. The interaction was evaluated by Western analysis (Santa Cruz; primary antibodies:  $G_{\alpha_q}$ , E-17 sc-393;  $G_{\alpha_o}$ , K-20 sc-387).
  42. Acetylcholine stimulation of Neuro-2A and PLC inhibition. Neuro-2A cells were plated in 24-well plates and transfected with either 100 ng of pGFPFLtub and 50 g of empty pCDNA vector, pCDNA(AChR-M1), or pCDNA(AChR-M2) with Effectene transfection reagent. Twenty-four hours after transfection the cells were washed with PBS and incubated with complete DMEM containing 100  $\mu$ M acetylcholine. Cover slips were processed at the specified times. Quantitation of cells containing nuclear tubby was performed with cells that were preincubated for 10 min at 37°C in either dimethyl sulfoxide (DMSO), 1  $\mu$ M U73122, or 1  $\mu$ M U73343 (dissolved in DMSO) (Calbiochem 662035 or 662041). Acetylcholine (100  $\mu$ M) was added to the cells, and the percentage of cells containing nuclear tubby was quantified.
  43. E. Kobrinisky, T. Mirshahi, H. Zhang, T. Jin, D. E. Logothetis, *Nature Cell Biol.* **2**, 507 (2000).
  44. D. Julius, A. B. MacDermott, R. Axel, T. M. Jessell, *Science* **241**, 558 (1988).
  45. B. L. Roth, D. L. Willins, K. Kristiansen, W. K. Kroeze, *Pharmacol. Ther.* **79**, 231 (1998).
  46. 5HT $_{2c}$  mutants. The following mutants of the 5HT $_{2c}$  receptor were tested for their capacity to induce nuclear translocation of tubby. These mutants are known to substantially abrogate the signaling function of 5HT $_{2c}$ : D135N, S139A, F3301L, I331L, W357A, and Y360A (45).
  47. S. Offermanns *et al.*, *EMBO J.* **17**, 4304 (1998).
  48. J. D. Vickers, *J. Pharmacol. Exp. Ther.* **266**, 1156 (1993).
  49. R. Kapeller *et al.*, *J. Biol. Chem.* **274**, 24980 (1999).
  50. J. S. Flier, E. Maratos-Flier, *Cell* **92**, 437 (1998).
  51. H. Ohki-Hamazaki *et al.*, *Nature* **390**, 165 (1997).
  52. D. Huszar *et al.*, *Cell* **88**, 131 (1997).
  53. A. S. Chen *et al.*, *Nature Genet.* **26**, 97 (2000).
  54. J. C. Erickson, K. E. Clegg, R. D. Palmiter, *Nature* **381**, 415 (1996).
  55. M. S. Szczycka *et al.*, *Proc. Natl. Acad. Sci. U.S.A.* **96**, 12138 (1999).
  56. L. H. Tecott *et al.*, *Nature* **374**, 542 (1995).
  57. X. Jian *et al.*, *J. Biol. Chem.* **274**, 11573 (1999).
  58. Y. Saito *et al.*, *Nature* **400**, 265 (1999).
  59. H. Y. Wang, A. S. Undie, E. Friedman, *Mol. Pharmacol.* **48**, 988 (1995).
  60. J. I. Hartman, J. K. Northup, *J. Biol. Chem.* **271**, 22591 (1996).
  61. K. Nonogaki, A. M. Strack, M. F. Dallman, L. H. Tecott, *Nature Med.* **4**, 1152 (1998).
  62. S. F. Leibowitz, J. T. Alexander, *Biol. Psychiatry* **44**, 851 (1998).
  63. P. M. Nishina, S. Lowe, J. Wang, B. Paigen, *Metabolism* **43**, 549 (1994).
  64. P. A. Sargent, A. L. Sharpley, C. Williams, E. M. Goodall, P. J. Cowen, *Psychopharmacol. Ser. (Berl.)* **133**, 309 (1997).
  65. A. T. Brunger, *X-PLOR, Version 3.1: A System for X-ray Crystallography and NMR* (Yale Univ. Press, New Haven, CT, 1992).
  66. A. T. Brunger *et al.*, *Acta Crystallogr. Sect. D Biol. Crystallogr.* **54**, 905 (1998).
  67. T. A. Jones, J. Y. Zou, S. W. Cowan, M. Kjeldgaard, *Acta Crystallogr.* **A47**, 110 (1991).
  68. W. He *et al.*, *Brain Res. Mol. Brain Res.* **81**, 109 (2000).
  69. S. V. Evans, *J. Mol. Graphics* **11**, 134 (1993).
  70. A. Nicholls, K. Sharp, B. Honig, *Proteins* **11**, 281 (1991).
  71. We thank M. Simon for the  $G_{\alpha_q}/G_{\alpha_{11}}$  double-knock-out cell line; R. Iyengar and D. Jordan for multiple G-protein reagents; F. Mancina and R. Axel for 3T3-5HT $_{2c}$  receptor cells and 5HT $_{2c}$  receptor cDNA; L. H. Wang for CHO-IR cells; and M. Goldfarb for tyrosine kinase receptor expression plasmids. Some of the cDNA clones for human G $\alpha$  proteins were provided by the Guthrie cDNA Resource Center ([www.guthrie.org/cdna](http://www.guthrie.org/cdna)). We also thank W. Hendrickson, R. Axel, A. Aggarwal, P. Kwong, R. Iyengar, D. Logothetis, and S. Aaronson for helpful comments on the manuscript, and C. Ogata and the staff of the NSLS beamline X4A for help with data collection. We are grateful to D. Colman and S. Aaronson for help with financial support. T.J.B. is the recipient of a Wellcome Trust International Prize Traveling Research Fellowship. S.S. was supported by a NIH postdoctoral training grant awarded to the Division of Nephrology, Department of Medicine, Mount Sinai School of Medicine. L.S. is the recipient of a Career Scientist Award from the Irma T. Hirsch and Monique Weill-Caulier Trust, and a Career Development Award from the American Diabetes Association. Beamline X4A at the NSLS, a U.S. Department of Energy facility, is supported by the Howard Hughes Medical Institute. Coordinates have been deposited in the Protein Data Bank (accession code 1I7E).

2 April 2001; accepted 10 May 2001

Published online 24 May 2001;

10.1126/science.1061233

Include this information when citing this paper.

## REPORTS

## Discovery of Hidden Blazars

Feng Ma<sup>1\*</sup> and Beverley J. Wills<sup>2</sup>

Every radio-loud quasar may have blazar activities, according to a unified scheme where the differences in both optical and radio observations of radio-loud quasars are the result of different viewing angles. We have predicted that blazars may be detected using emission line ratio variations caused by variable illumination of gas clouds in the broad emission line region. In a spectroscopic search of 62 quasars at a redshift of about 2, we have discovered large (>20%) variations of the emission line ratios, CIV/CIII] or CIV/Ly $\alpha$ , when compared with data taken more than 10 years ago. This result is consistent with our prediction and supports the unification scheme for radio-loud quasars.

Quasars are the most luminous of active galactic nuclei (AGN). About 10% of all cataloged quasars are more luminous at radio

than at optical wavelengths, and thus are classified as radio-loud quasars. Their strong radio emission arises from two jets shooting away from the center in opposite directions, terminating in extended radio lobes. It is believed that massive black holes and accretion disks are the central engines of all quasars (1, 2). However, it is unclear what gives rise to the powerful radio jets. It may be that these

jets are produced in the vicinity of only the most massive black holes (3), or perhaps in those with greatest angular momentum (4).

Radio-loud quasars are not all alike. However, the diversity in their radio structures and optical spectra can be explained by a unified scheme based on the viewing angle (5, 6). If we look directly into the jet, we see strongly beamed synchrotron radiation with the energy distribution peaking in the infrared wavelength. This synchrotron radiation is highly variable and often dominates the light from the quasar's accretion disk and broad emission lines. An object with these characteristics is classified as a blazar. If the line of sight is a few degrees away from the jet direction, we can still see a bright radio core, which dominates the radio power, and this quasar is classified as core-dominant. As the viewing angle is increased beyond a few degrees to the jet direction, the beamed synchrotron emission in radio through optical wavelengths dims. When the jet-lobe structure is viewed at a larger angle, the infrared through

<sup>1</sup>Prc-Mrc 2nd Floor/R9950, <sup>2</sup>McDonald Observatory and Astronomy Department, University of Texas, Austin, TX 78712, USA.

\*To whom correspondence should be addressed. E-mail: feng@astro.as.utexas.edu

optical emission is dominated by thermal accretion continuum and broad emission lines, and the radio core becomes less bright than the radio lobes. These are the lobe-dominant quasars. As the viewing angle is further increased, the quasar continuum and broad line emission are hidden behind an almost edge-on thick dusty nuclear torus or dust in the host galaxy. The only clue to a hidden quasar may be the extended jets and radio lobes. Observationally, this is a radio galaxy.

If the unified scheme (5, 6) is correct, every radio-loud quasar should harbor a blazar, and we may be able to observe signatures of the hidden blazars. Our models have shown that the large flux of beamed infrared radiation from a hidden blazar can heat the broad emission line region (BELR) gas, enhancing collisionally excited emission lines such as CIV (154.9 nm) and SiIV (139.7 nm) (7). A key signature of this variable heating would be large variations of the line intensity ratios, CIV/Ly $\alpha$  or CIV/CIII], because Ly $\alpha$ , CIII] (190.9 nm), and all Balmer lines are much less affected by the heating. The latter lines are more sensitive to hydrogen-ionizing ultraviolet photons that are scarce in the beamed steep-spectrum synchrotron radiation.

A large blazar outburst may occur once every 10 to 20 years. For example, 3C 279 showed one outstanding outburst in each of two 20-year monitoring periods (8), and each of the outbursts lasted for about 1 year. During the outbursts, this blazar was more than 15 times as bright as usual. Smaller amplitude (factor of 2) variations are also common when this blazar is not in outburst. If every radio-loud quasar harbors a 3C 279-type blazar, then in each case we would expect to see variations of emission line equivalent width (EW) ratio (CIV/CIII] or CIV/Ly $\alpha$ ) larger than 20% once every  $\sim$ 60 years in the observer's frame (for redshift  $z \sim 2$ , in order for the ultraviolet emission lines to redshift into the optical wavelength range, and taking into account a  $1 + z$  time dilation factor). Instead of monitoring a few quasars for so many years to look for the predicted line ratio variations, we use an alternative approach—comparing new spectra from a sample of 62 radio-loud quasars with historical spectra taken more than 10 years ago. The quasars in our sample have a redshift  $1 < z < 3$  and absolute magnitudes  $-31 < M_B < -25$ . Because 3C 279 spent  $\sim$ 5% of its lifetime in outburst, we would expect to catch three outbursts in our sample during each of the two epochs, or six events with EW CIV/CIII] or EW CIV/Ly $\alpha$  variations larger than 20%. The large range in blazar luminosity and variability suggests that the event rate may be higher or lower than estimated here.

Earlier studies of AGN variability have focused on nearby, low-luminosity, radio-weak objects with known continuum variability. One such object is NGC 5548, for which Ly $\alpha$ , CIV, and CIII] lines have been found to

vary with similar amplitudes in response to variations of the normal, nonsynchrotron continuum (which may arise in an accretion disk, for example) (9). The amplitude of line variations is usually less than half that of the continuum; this is also true for Balmer lines in a sample of low-redshift ( $z \sim 0.1$ ) quasars (10, 11) and in a sample of radio-loud ( $z = 0.14$  to  $0.59$ ) quasars, including both core-dominant and lobe-dominant objects (12). Systematic spectroscopic monitoring of luminous high-redshift quasars has not been done before. Photometric studies of large samples of quasars indicate that those of higher luminosity are less variable (13–15). For a quasar in the luminosity range of our sample ( $-31 < M_B < -25$ ), when measured at two epochs, the typical variation is less than 0.2 magnitude (13, 14). The expected emission line variations are  $< 10\%$  in response to a 0.2-magnitude normal continuum variation. The line ratio variations are even smaller (9, 16).

Most of the new spectra were obtained from 1998 to 2000 using the Large Cassegrain Spectrograph on the 2.7-m Harlan J. Smith telescope at McDonald Observatory. We typically used a 2-arc sec slit for long exposures (e.g., 5400 s for objects of 18.5 visual magnitude), followed by a short (600-s) exposure with a wide slit (8 arc sec) to correct the narrow-slit spectra. The seeing was typically 2 to 3 arc sec, and thus an 8-arc sec slit exposure is sufficient to correct the shape of narrow-slit spectra for atmospheric refraction losses. During each night, usually five standard stars were observed using the 8-arc sec slit to calibrate quasar continuum shapes. Each spectrum was calibrated for wavelength with the use of argon and neon lamps. Many spectra were taken under non-photometric conditions and thus are not on an absolute flux density scale.

Most of the historical spectra we used, such as those from (17), were obtained using narrow slits and are not absolutely flux-calibrated. Hence, we focus on comparing emission line EW ratio variations. We used direct division of two spectra to reveal the variability of emission lines relative to the local

continuum [e.g., (18)]. A featureless division spectrum indicates that there are probably no variations in the continuum or emission lines, because terrestrial clouds only cause a gray suppression of the spectra, and wavelength-dependent slit losses resulting from atmospheric dispersion cause a low-order continuum shape difference. We divide spectrum 1 at one epoch by spectrum 2 at another epoch; avoiding regions of emission lines, we fit a low-order curve to this division spectrum, and multiply spectrum 2 by this curve. Thus, we normalize the continua, removing the effects of wavelength-dependent continuum variation. Information about changes in the ratios of emission line strengths is preserved unless there is a real variation in the continuum shape. Very little is known about how the continuum shape varies in a quasar spectrum. However, some clues can be inferred from NGC 5548, which is  $\sim 17\%$  more variable at 135.0 nm than at 184.0 nm in the rest frame while the average continuum variation amplitude is a factor of 2 (15). This would cause a 17% apparent emission line EW ratio (Ly $\alpha$ /CIII]) variation in our method of analysis. We note that quasars in our sample are much less variable than NGC 5548, and hence, the continuum shape variation is probably less than 17%.

For half of the objects in our sample, the spectra at the two epochs match well (Table 1, class C). This is consistent with photometric findings that quasars at this redshift and luminosity range are generally not highly variable, so our comparison method appears tenable. Most of the class D objects, which are core-dominant and known to be more variable than lobe-dominant objects (18), could cause the apparent proportional line variations if our method of comparison is used. Large line variations are seen only in CIV lines (Fig. 1), consistent with our predicted behavior for quasars with hidden blazars.

MRC 0238+100 [ $z = 1.83$  (17),  $M_B = -27.7$  (19)] shows an increase of 70% in its CIV line strength between 2 December 1986 and 10 November 1999. A SiIV (139.7 nm)

**Table 1.** Classification of emission line EW ratio variability in the sample. Column 2 gives the number of objects in each class; the number of core-dominant objects is given in parentheses.

Class	Number	Description	Interpretation
A	3 (1)	Large relative CIV variations ( $> 20\%$ )	Outbursting hidden blazars revealed
B	9 (3)	Smaller relative CIV variations (10 to 15%)	Hidden blazars active
C	33 (7)	No variations $> 10\%$ in any lines	High- $z$ and high-luminosity quasars not very variable
D	15 (10)	All lines vary in proportion	Continuum variation at different epochs; emission line response to normal quasar continuum
E	2 (1)	Variations of 10 to 15% in Ly $\alpha$ but not CIV	Continuum more variable in the blue than in the red

REPORTS

line, not present in the historical spectrum, appeared in our new spectrum. The SiIV line is more sensitive than the CIV line to infrared heating, and the intensity of the SiIV line may increase by 100% according to our models (7). The appearance of the SiIV line in our new spectrum suggests that the CIV enhancement is due to infrared heating from the additional blazar continuum. The low signal-to-noise ratio near the CIII] line means that we can only constrain the CIII] variation to be <30%. Hence, the variation in emission line EW ratio in this case is >30% for CIV/CIII] over the time interval of 13 years. From the digitized (red plate) Palomar observatory sky surveys I and II (20), we find for MRC 0238+100 a differential variation of  $0.01 \pm 0.20$  magnitude between epochs 1954 and 1990. Comparing our four new observations on 22 November 1998, 10 November 1999, 2 March 2000, and 1 January 2001—a time interval of 2.1 years (or 0.74 years in this quasar’s rest frame)—reveals no large continuum or emission line variations. We suggest that the hidden blazar inside MRC

0238+100 is currently in an outburst, maintaining strong CIV and SiIV line emission with little change in the observed continuum or CIII] emission line. The low-activity state of the hidden blazar in 1986 is supported by an earlier observation in 1976 (21), when MRC 0238+100 had line-to-continuum ratios (defined as flux ratios from the line peak to the continuum level; unfortunately, the spectrum was not published) of 2.50 for CIV and 1.53 for CIII]. These observed line strengths are consistent with the 1986 values, whereas in our new spectrum the line-to-continuum ratios are 3.8 for CIV and 1.6 for CIII], as can be measured from Fig. 1.

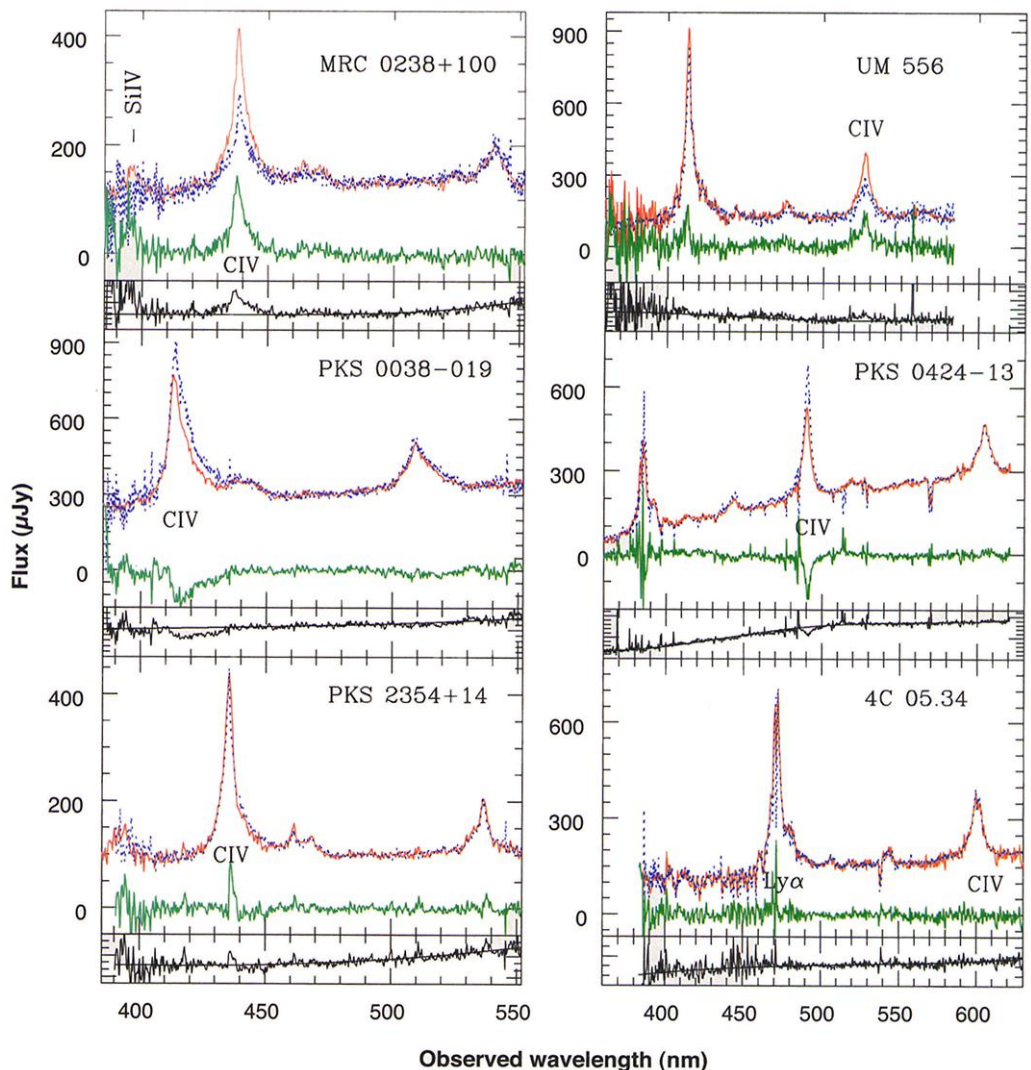
UM 556 [ $z = 2.39$ ,  $M_B = -28.4$  (19)] shows an increase of 70% in its CIV line strength between 6 March 1988 and 5 June 2000. The Ly $\alpha$  line is  $\sim 10\%$  stronger in 2000 than in 1988. The SiIV line also appears to be stronger in 2000, but with less certainty because it is a weak line in these spectra. The line EW ratio variation is thus 55% for CIV/Ly $\alpha$ .

If we assume that the blazar outbursts do

not last longer than 1 year in the rest frame, as suggested by observations of nearby blazars, we can predict that the CIV line in MRC 0238+100 and UM 556 will drop significantly within the next 3 years. Even though the hidden blazar’s continuum may vary on time scales of less than several months or even days, the observed emission lines are unlikely to vary on these time scales, because the light travel time across the BELR [several light months in high-luminosity quasars (11)] will result in the smearing of such variations.

PKS 0038–019 [ $z = 1.67$  (17),  $M_B = -26.9$  (19)] shows a CIV line 43% stronger in 1986 than in 1999, whereas its CIII] line is 18% stronger in 1986 than in 1999. The line EW ratio (CIV/CIII]) in 1986 is thus 21% larger than in 1999. The emission line intensity variation of CIV is seen in the red wing, suggesting that the part of BELR gas in the beam is moving away from us. This shows the potential of the technique to probe the polar regions of the quasar BELR. However, this case is not as convincing as in MRC 0238+100 because there is uncertainty in matching the continuum

**Fig. 1.** Comparison of spectra at two epochs. The continua at different epochs have been scaled to the same level. Red solid lines are new spectra taken from 1998 to 2000. Blue dotted lines are historical spectra taken from 1986 to 1988. Subtraction spectra (green lines) are plotted in the same panels. The flux level is plotted in  $\mu\text{Jy}$  [ $1 \text{ jansky (Jy)} = 10^{-26} \text{ W m}^{-2} \text{ Hz}^{-1}$ ]. In the lower portion of each panel, the division spectra (before scaling) and the fitting curves are plotted together in arbitrary units.



at the blue end of the spectra, and because the historical spectrum did not include the SiIV line. We also derive from the digitized Palomar Observatory sky surveys (20) a differential photometric variation of  $0.11 \pm 0.45$  magnitude. The large error bar may be due to the plate quality and the slight difference in the band-passes at the two epochs.

For PKS 0424-13 [ $z = 2.17$ ,  $M_B = -28.6$  (19)], the spectrum obtained on 16 February 1990 shows the CIV line to be 25% stronger than on 20 December 1998, whereas Ly $\alpha$  is ~10% stronger in 1990 than in 1998. The line EW ratio CIV/Ly $\alpha$  is thus 14% larger in 1990 than in 1998. In addition, the CIII] line shows little variation in this object. The CIV line variation is thus constrained from both ends of the spectrum, ruling out the possibility that the observed line variation is caused by continuum shape variation in this object.

Both MRC 0238+100 and PKS 0038-019 are lobe-dominant with clear double-lobed radio structures (22). The ratios of core to total radio flux density of MRC 0238+100 and PKS 0038-019 at rest frame 5 GHz are 0.098 and 0.067, respectively (23). The lobe-dominant radio structure of PKS 0424-13 is implied by its steep radio spectrum (24). We do not expect to see the variable blazar continuum at such large implied viewing angles away from the beam. Although some large apparent emission line variations have been reported in core-dominant quasars with large continuum variations [e.g., an EW change of 68% in CIV and 82% in CIII] for 3C446 (18)], no large line ratio variations comparable to the cases of MRC 0238+100 and UM 556 have been reported so far, except for the low-luminosity AGN NGC 5548 [e.g., (25), where a HeII (468.6 nm) flare was interpreted as an accretion event]. We also note that because 90% of quasars are radio-quiet, some of them have inevitably been observed more than once, yet no large line ratio variations have been published (26).

Our observations offer support for the unified scheme for radio-loud quasars. The emission line variations provide the most direct evidence for the existence of violent blazar outbursts in every radio-loud quasar. Similar ideas can be applied to other jet-disk systems such as gamma-ray bursts and protostars. In addition, the disk-wind model for the broad line-emitting clouds, with the winds blowing off the accretion disk by radiation pressure (27), is challenged because it does not include any gas in the polar regions. Another widely adopted model, the stellar atmosphere model for the BELR (28), has been challenged by emission line profile studies (29). Hence, other explanations for the origin of BELR gas may be needed. Finally, our results suggest that radio-loud quasars should be excluded when studying cosmology via the Baldwin effect [the inverse

relation between EW (CIV) and continuum luminosity (30)]. Reducing the scatter in this relation is critical for using quasars as luminosity indicators (31), whereas radio-loud quasars introduce extra scatter as a result of their hidden blazar activity.

References and Notes

1. J. G. Hills, *Nature* **254**, 295 (1975).
2. G. A. Shields, *Nature* **272**, 706 (1978).
3. A. Laor, *Astrophys. J.* **543**, L111 (2000).
4. R. D. Blandford, R. L. Znajek, *Mon. Not. R. Astron. Soc.* **179**, 433 (1977).
5. R. Antonucci, *Annu. Rev. Astron. Astrophys.* **31**, 473 (1993).
6. C. M. Urry, P. Padovani, *Pub. Astron. Soc. Pac.* **107**, 803 (1995).
7. F. Ma, B. J. Wills, *Astrophys. J.* **504**, L65 (1998).
8. J. R. Webb et al., *Astron. J.* **100**, 1452 (1990).
9. S. Kaspi, H. Netzer, *Astrophys. J.* **524**, 71 (1999).
10. D. Maoz, P. S. Smith, B. T. Jannuzi, S. Kaspi, H. Netzer, *Astrophys. J.* **421**, 34 (1994).
11. S. Kaspi et al., *Astrophys. J.* **533**, 631 (2000).
12. M. R. Corbin, P. S. Smith, *Astrophys. J.* **532**, 136 (2000).
13. I. M. Hook, R. G. McMahon, B. J. Boyle, M. J. Irwin, *Mon. Not. R. Astron. Soc.* **268**, 305 (1994).
14. S. Cristiani et al., *Astron. Astrophys.* **306**, 395 (1996).
15. M. R. S. Hawkins, *Astron. Astrophys.* **143**, 465 (2000).
16. J. C. Shields, G. J. Ferland, B. M. Peterson, *Astrophys. J.* **441**, 507 (1995).
17. P. D. Barthel, D. R. Tytler, B. Thomson, *Astron. Astrophys. Suppl. Ser.* **82**, 339 (1990).
18. E. Pérez, M. V. Penston, M. Moles, *Mon. Not. R. Astron. Soc.* **239**, 55 (1989).
19. M. P. Véron-Cetty, P. Véron, *ESO Sci. Rep.* **17** (1996).
20. I. N. Reid et al., *Pub. Astron. Soc. Pac.* **103**, 661 (1991).

21. S. Mitton, C. Hazard, J. A. J. Whelan, *Mon. Not. R. Astron. Soc.* **179**, 569 (1977).
22. P. D. Barthel, G. K. Miley, R. T. Schilizzi, C. J. Lonsdale, *Astron. Astrophys. Suppl. Ser.* **73**, 515 (1988).
23. K. Nilsson, *Astron. Astrophys. Suppl. Ser.* **132**, 31 (1998).
24. P. D. Barthel, G. K. Miley, *Nature* **333**, 319 (1988).
25. B. M. Peterson, G. J. Ferland, *Nature* **324**, 345 (1986).
26. T. Small, W. L. W. Sargent, and C. C. Steidel [*Astron. J.* **114**, 2254 (1997)] reported a large apparent CIV emission line variation in the radio-quiet quasar Q 0946+3009 from 1990 to 1992. However, in their analysis of the spectra, rather subjectively chosen continua at the two epochs were used and were subtracted from the original data. By reanalyzing their original data using our method, we found no CIV emission line variation [F. Ma, thesis, University of Texas at Austin (2000)]. Undulations in the division spectrum are seen and are probably the result of calibration errors.
27. N. Murray, J. Chiang, S. A. Grossman, G. M. Voit, *Astrophys. J.* **451**, 498 (1995).
28. T. Alexander, H. Netzer, *Mon. Not. R. Astron. Soc.* **270**, 781 (1994).
29. N. Arav, T. A. Barlow, A. Laor, W. L. W. Sargent, R. D. Blandford, *Mon. Not. R. Astron. Soc.* **297**, 990 (1998).
30. J. A. Baldwin, *Astrophys. J.* **214**, 679 (1977).
31. J. Baldwin, in *Quasars and Cosmology*, G. Ferland, J. Baldwin, Eds. (Astronomical Society of the Pacific, San Francisco, 1999), p. 475.
32. We thank J. Baldwin, P. Barthel, P. Francis, T. Small, M. Vestergaard, and J. Yuan for making their data available in digital form; G. Shields for helpful discussions; D. Wills for help with the manuscript; and D. Doss and M. Prado for their supporting work at McDonald Observatory. This work makes use of the Space Telescope Science Institute (STScI) Digitized Sky Survey and the NASA/IPAC Extragalactic Database (NED).

5 March 2001; accepted 7 May 2001

# Observation of Magnetic Hysteresis at the Nanometer Scale by Spin-Polarized Scanning Tunneling Spectroscopy

O. Pietzsch,\* A. Kubetzka, M. Bode, R. Wiesendanger

Using spin-polarized scanning tunneling microscopy in an external magnetic field, we have observed magnetic hysteresis on a nanometer scale in an ultrathin ferromagnetic film. An array of iron nanowires, being two atomic layers thick, was grown on a stepped tungsten (110) substrate. The microscopic sources of hysteresis in this system—domain wall motion, domain creation, and annihilation—were observed with nanometer spatial resolution. A residual domain 6.5 nanometers by 5 nanometers in size has been found which is inherently stable in saturation fields. Its stability is the consequence of a 360° spin rotation. With magnetic memory bit sizes approaching the superparamagnetic limit with sub-10 nanometer characteristic lengths, the understanding of the basic physical phenomena at this scale is of fundamental importance.

The investigation of magnetic nanostructures has been hampered by the lack of magnetic imaging techniques with an adequate spatial

resolution [for an overview on the relevance of such structures see, e.g., (1)]. A scanning tunneling microscope is expected to be the ultimate microscopic magnetic investigation tool if the tip itself is a source of spin-polarized electrons (2). First reports on spin-polarized scanning tunneling microscopy (SP-STM) 10 years ago (3, 4) have shown that the use of magnetic probe tips provides

Institute of Applied Physics and Microstructure Research Center, University of Hamburg, Jungiusstrasse 11, D-20355 Hamburg, Germany.

\*To whom correspondence should be addressed. E-mail: pietzsch@physnet.uni-hamburg.de